Optical and Quantum Electronics (2006) 38:557–566
DOI 10.1007/s11082-005-4699-y

Robust 2 × 2 multimode interference optical switch

D. A. MAY-ARRIOJA*, N. BICKEL AND P. LIKAMWA
College of Optics and Photonics: CREOL & FPCE, University of Central Florida, P.O. Box 162700, Orlando, FL 32816-2700, USA
*(*author for correspondence: E-mail: may@creol.ucf.edu)*

Received 13 June 2005; accepted 2 November 2005

Abstract. A robust 2 × 2 photonic switch based on multimode interference (MMI) effects is proposed. We demonstrate that the device is very tolerant to material modifications and typical fabrication errors. This is a result of the MMI design and the high symmetry of the switch. The key parameter for the operation of the device is that the input light forms a pair of well defined self-images exactly in the middle of the switch. The index modulated regions precisely overlap the positions where these two self-images are formed. By creating identical contact features at these locations, any refractive index change induced in the material as a result of electrical isolation will be replicated in both self-images, and therefore the off-state output will not be altered. In the same way, offset and dimension errors are reflected symmetrically on both self-images and do not seriously affect the imaging. The characteristics of the switch under different scenarios are investigated using the finite difference beam propagation method. By employing this configuration, crosstalk levels better than −20 dB are achievable over a wavelength range of 100 nm while maintaining polarization independence.

Key words: electrooptic, integrated optics, multimode interference, photonic switch, polarization independent, semiconductor

1. Introduction

The use of multimode interference (MMI) effects for the development of passive integrated devices has been widely investigated. They have attracted a great deal of interest because they offer several advantages, such as very compact devices, low polarization sensitivity, and relaxed fabrication tolerances (Soldano and Pennings 1995; Levy *et al.* 1999; Themistos and Rahman 2002). Recently, their use has been expanded from passive to active devices, and several photonic switches have been proposed using MMI effects (Yagi *et al.* 2000; Leuthold and Joyner 2001; Earnshaw and Allsopp 2002; Lien *et al.* 2002; Nagai *et al.* 2002). The switching mechanism of these MMI-based switches is quite similar. They operate by modifying the refractive index at specific areas within the MMI waveguide, which are collocated with the occurrence of multiple self-images. This change in the refractive index effectively alters the phase relation between the self-images, which leads to a modified output image and switches the light between the output waveguides.

These configurations are of great interest, since, in principle, very efficient switching can be achieved. However, in order to have access to the large refractive index change required for switching ($\Delta n = 3 \times 10^{-2}$), the devices must rely on the principle of carrier induced refractive index change in semiconductors. Therefore, electrical current injection is required for the device operation, and this requirement imposes some restrictions on the device design. Since the index change is assumed to occur at a very precise region within the MMI waveguide, any excessive current spreading will seriously deteriorate the switching performance (Leuthold and Joyner 2001; Nagai *et al.* 2002). It is then necessary to electrically isolate the index modulated regions from the rest of the MMI waveguide. Several techniques are currently available, such as proton implantation and zinc in-diffusion. Zinc in-diffusion is particularly attractive since it has been widely used for the fabrication of optoelectronic devices (Nagai *et al.* 1995; Yang *et al.* 1995; Yun and Hyun 2000). We have also demonstrated that current spreading can be regulated by carefully controlling the zinc diffusion depth (May-Arrioja *et al.* 2005). In order to restrict the current spreading as much as possible, the zinc has to diffuse to a depth that is very close to the guiding layer. The only drawback of using this approach is that, even in the absence of an injected current, an effective refractive index change is induced beneath the zinc diffused areas (Ito *et al.* 1989). This could modify the imaging conditions of the MMI waveguide, which in turn would deteriorate the crosstalk of the device. A similar effect has also been observed when using proton implantation, due to the difference in the built-in electric field between implanted and un-implanted sections (Huang *et al.* 1993). Ideally, the contacts used for current injection should have the same dimensions as the index modulated regions. However, a small amount of current leakage can be expected regardless of the isolation technique. Therefore, the width of the index modulated region will always be wider than that of the contact. Consequently, the term 'contact' hereafter refers to the region that was electrically isolated, and 'index modulated region' refers to the area defined by the injected current.

Interestingly, no analysis has been previously carried out regarding the device performance as a function of the deviation from the optimum dimensions of the index modulated regions. In fact, contact width reduction might be required in order to isolate adjacent contacts, and also to achieve better definition of the index modulated regions. This, however, will create finite sections within the MMI waveguide that possess an effective index change, which can lead to deterioration of the switch crosstalk. Moreover, during device fabrication, we often have to deal with offset errors resulting from the misalignment between different masking layers. Such a displacement of the index modulated regions, with respect to the optimum positioning, is potentially a very serious issue. This offset error may lead to

an imbalance in the phase of the adjacent self-images, thereby making it impossible to achieve the phase difference required for switching. An error of this type would manifest as an increase in the switching crosstalk. It is therefore very important to address these issues during the design of an MMI-based switch.

In this paper we propose a highly robust 2×2 MMI-based photonic switch. We demonstrate that the device is very tolerant to material modifications and typical fabrication errors. This is a result of the MMI design and the high symmetry of the switch. The characteristics of the switch under different scenarios are investigated using the finite difference beam propagation method (FDBPM). For this configuration, crosstalk levels better than -20 dB can be achieved over a wavelength range of 100 nm, while still maintaining polarization independence.

2. Switch Design

A schematic of the proposed switch is shown in Fig. 1. The device consists of a MMI waveguide with a width of $W = 18\,\mu$m and a length of $L = 998\,\mu$m. Light is launched using $3\,\mu$m wide input and output waveguides that are separated by $3\,\mu$m. The shaded zones correspond to the index modulated regions. The dimensions of the MMI switch were calculated using the well known relations for paired restricted interference in MMI waveguides (Soldano and Pennings 1995). The length is set to $L\pi$ (where $L\pi$ corresponds to the beat length) such that light coupled to the upper input waveguide will be imaged into the lower output waveguide during the off-state, as shown in fig. 2(a). The device is modeled using a $1\,\mu$m thick InGaAsP guiding layer ($\lambda_g = 1.3\,\mu$m) with a $1.5\,\mu$m thick InP top cladding layer. The refractive indices of the layers are 3.41 and 3.17 respectively.

The key parameter for the operation of the device is that the input light forms a pair of well defined self-images exactly at the middle of the switch, and along the central axis of both access waveguides, as shown in Fig. 2(a).

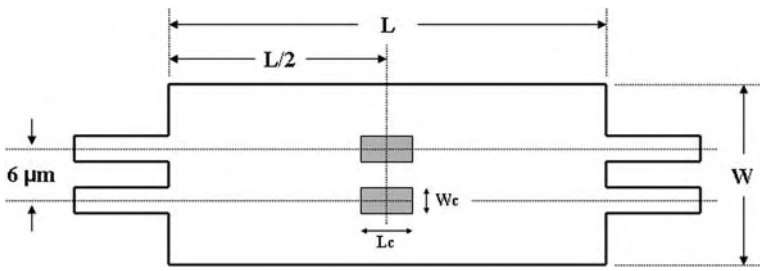

Fig. 1. Schematic of the 2×2 photonic switch and design parameters.

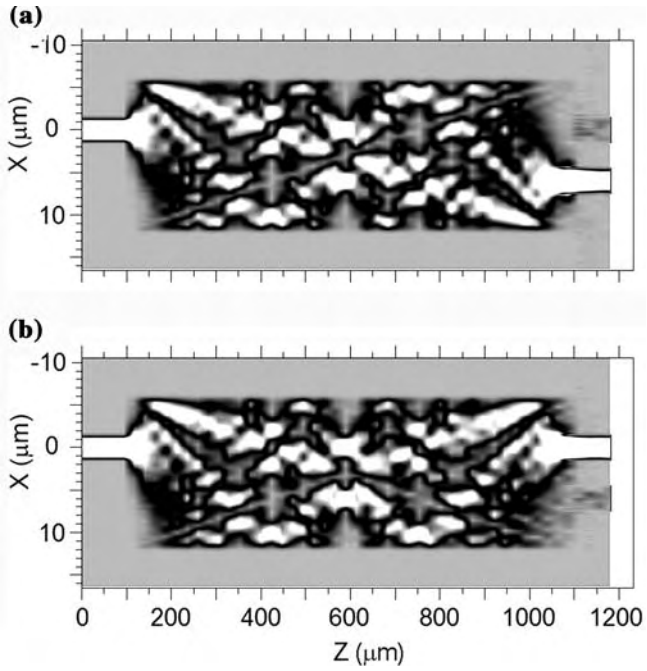

Fig. 2. Beam propagation characteristics (a) Without index modulation, and (b) With π phase shift applied to lower index modulated region.

The index modulated regions precisely overlap the positions where these two self-images are formed. By creating identical features at these locations, any refractive index change induced in the material as a result of electrical isolation will be reflected in both self-images, and therefore the off-state output will not be altered. In the same way, offset and dimension errors are reflected symmetrically on both self-images and the imaging is not seriously affected. It is important to note that, in the on-state, only one of the index modulated regions will be active.

The operation of the switch is quite simple. In the absence of an applied current, light coupled to the upper input waveguide is emitted from the lower output waveguide, and vice-versa. However, when a π phase shift is applied to either one of the index modulated regions, light coupled to the upper input waveguide will be imaged onto the upper output waveguide, as shown in Fig. 2(b). A similar performance is achieved for light coupled to the lower input waveguide. A maximum refractive index change of 1% was assumed as a result of current injection. This amount of index change has been theoretically and experimentally demonstrated in bulk InGaAsP semiconductors (Amann *et al.* 1989; Bennett *et al.* 1990; Schraud *et al.* 1991; Nagai *et al.* 2002), with an even stronger effect observed when multiple

quantum wells are employed (Shim *et al.* 1995). The dimensions of the index modulated regions were selected so as to obtain the lowest possible crosstalk for both TE and TM polarizations at a wavelength of 1.55 μm. In this case, an optimum width and length of $Wc = 3.5$ and $Lc = 28\,\mu$m were calculated, respectively.

3. Analysis

The performance of the switch was investigated using the FDBPM method. In the following simulations, an induced refractive index change of $\Delta n_1 = 1 \times 10^{-2}$ was assumed for both contacts as a results of contact isolation (Huang *et al.* 1993). This value is slightly higher than what we could normally expect, but it helps to demonstrate that the device is exceedingly tolerant to such effects. We also included in the simulations the intrinsic propagation loss of $5\,\text{cm}^{-1}$, as well as an increase in the absorption losses for the index modulated areas due to carrier injection (Nagai *et al.* 2002). The analysis considered a combination of effects that can lead to deterioration of the optimum crosstalk for each switching state. Here we define the switch crosstalk as the ratio of the residual optical power on the adjacent waveguide relative to the power on the desired waveguide, expressed in decibels (dB).

During the off-state, we were mainly concerned about modifications to the imaging due to Δn_1 variance induced through contact isolation. As we explained before, reduction of the contact size might be a necessary step in keeping the injected current within the optimum calculated value for the index modulated region. However, this reduces the area that is affected by Δn_1, which could have a detrimental effect during the off-state operation. The contact width (Wc) was then modified from 1.5 to 3.5 μm, and the off-state crosstalk was calculated for each case. As shown in Fig. 3, as the contact width is reduced, the induced perturbation Δn_1 stays entirely within the image, and has a negligible effect on the off-state crosstalk. In addition, we included lateral offset errors that are typically encountered during device fabrication. Currently, this value can be easily controlled within $+/-0.5\,\mu$m. Shown in Fig. 4 is the off-state crosstalk for different contact widths as a function of the offset error along both directions. As expected, there is an increase in the crosstalk as the contact is shifted from its nominal position. However, even when the contact width is reduced to 1.5 μm, and shifted by $+/-0.5\,\mu$m, the crosstalk is still better than $-35\,$dB. It can also be observed that the response is more symmetric as the contact width is reduced. This is due to the fact that a narrower contact will remain within the image, even when the offset is applied. Offsetting a wider contact generates an asymmetric phase shift in the images, and therefore, the response becomes asymmetric with respect to the offset position.

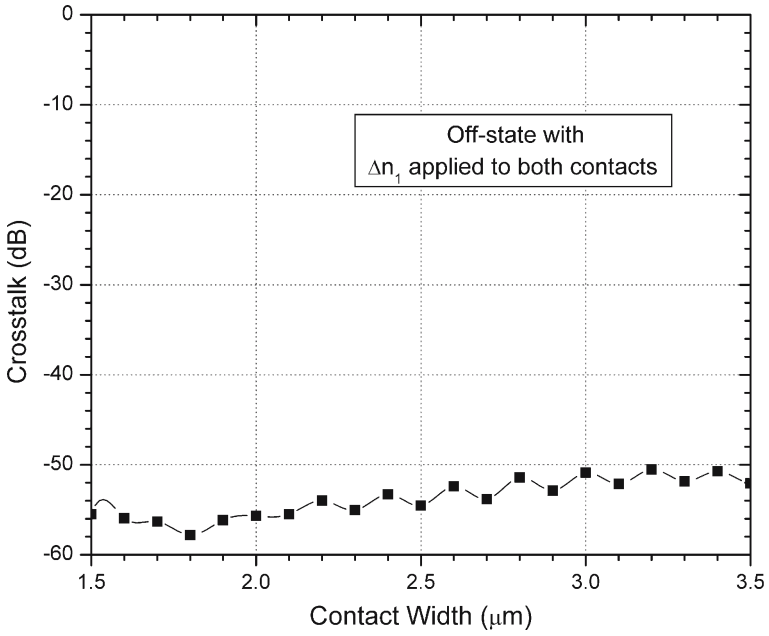

Fig. 3. Off-state crosstalk as a function of contact width.

Unexpectedly, there is a position for $Wc = 3.5\,\mu$m at which the crosstalk is slightly lower than that calculated for the nominal position. Nevertheless, the selected nominal position provides the best switching performance when wavelength and polarization dependence are considered. The low crosstalk levels obtained during the off-state are a direct consequence of using wide access waveguides ($3\,\mu$m) with a large separation between them ($3\,\mu$m), combined with a $1\,\mu$m thick waveguiding layer.

During the on-state, the major issue of concern is whether the injected current will be confined within the optimum index modulated region. As previously mentioned, regardless of the isolation technique, we can always expect a slight current leakage that will effectively increase the width of our contact. Therefore, it is important to determine the effects of increasing the width of the index modulation region. We define the effective index modulated width as $Wi = Wc + \Delta W$, where Wc corresponds to the optimum contact width of $3.5\,\mu$m and ΔW represents the amount of current spreading, namely $0\,\mu$m, $1\,\mu$m, and $2\,\mu$m. As shown in Fig. 5, increasing this width has only a minor effect on the on-state crosstalk, with the value maintained below -30 dB. For completeness, the added effects of offset errors were considered, and the resulting crosstalk characteristics are shown in Fig. 6. In this case, we can see that the device becomes less sensitive to offset errors as the width of the modulated regions is increased. This is

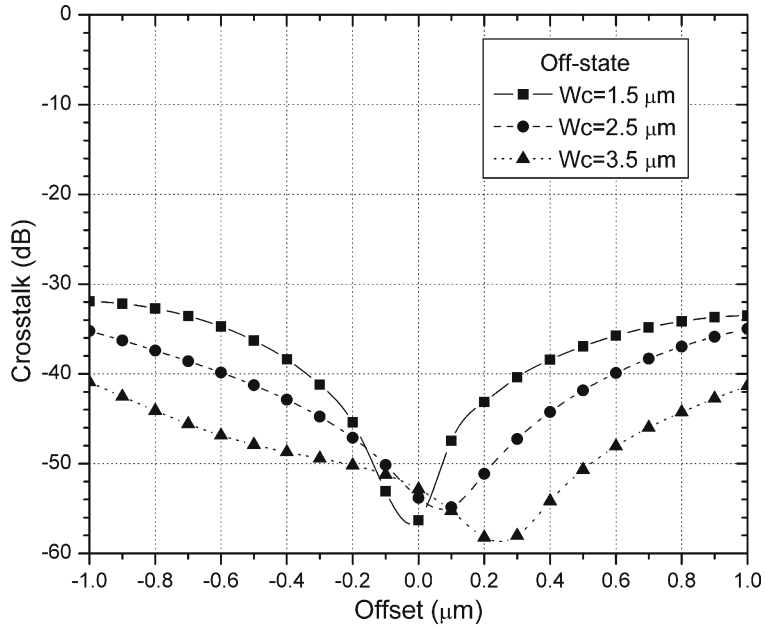

Fig. 4. Off-state crosstalk for different contact widths as a function of lateral offset.

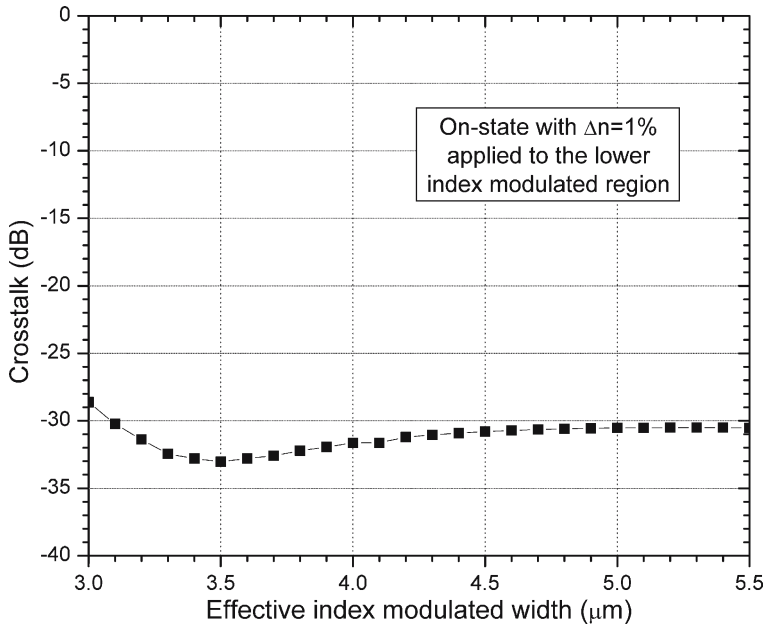

Fig. 5. On-state crosstalk as a function of effective index modulated width.

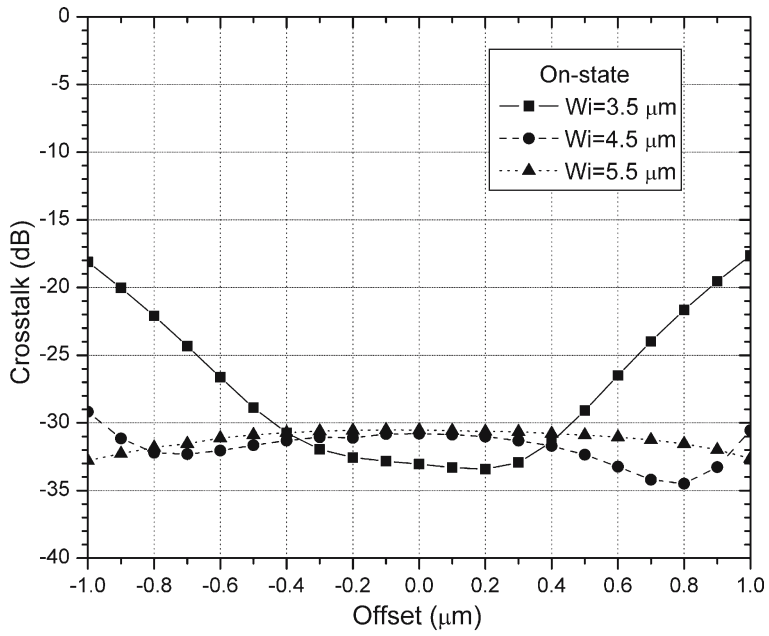

Fig. 6. On-state crosstalk for different effective index modulated widths as a function of lateral offset.

expected because, even though the modulated width is increased, the phase shift is still applied over the whole image whether offsets are present or not. This robustness is a direct result of the switch's high symmetry, and consequently, typical lateral offset errors can be considered negligible for this operational state.

The wavelength and polarization response of the switch were also investigated. In this case, the wavelength was scanned from 1.45 to 1.65 μm for both TE and TM polarizations, and for both states of operation. As shown in Fig. 7, there is a 100 nm window within which the crosstalk can be maintained below -20 dB for both polarizations. The switching speed is initially limited by depletion of the injected carriers (typically within the nanosecond range). However, this restriction could be removed by taking advantage of the remarkable symmetry exhibited by the device. A way to overcome the carrier lifetime limitation is to sweep out the injected carriers from the active region. This has generally been accomplished by reverse biasing the active region (Duthie *et al.* 1991; Angulo Barrios *et al.* 2003). In our device, both contacts can be reverse biased during the off-state without a major change in the off-state crosstalk, and with very low power consumption. During the on-state, one of the contacts is forward biased such that the light is switched. After the switching is completed, the contact is reverse

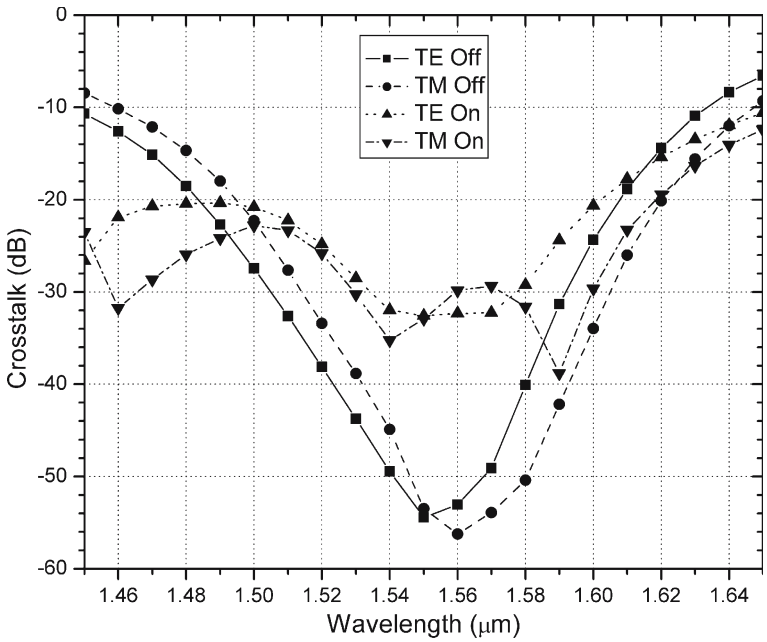

Fig. 7. Wavelength and polarization dependence of switch crosstalk for both operation states.

biased so that the carriers are swept out of the active region, thus allowing a faster transition between the on and off states.

From these results, it is clear that contact dimensions can be modified as needed to optimize the index modulated region. For instance, any excessive current spreading can be mitigated by reducing the contact width without any deterioration of the switch performance. This allows the possibility of using very simple isolation techniques, such as zinc in-diffusion, for the fabrication of high performance photonic switches. Finally, it should be noted that the length of the switch can be reduced by narrowing the width of the MMI region. However, the switch becomes more sensitive to the issues that we previously discussed, and this leads to a deterioration of the crosstalk, and a narrowing of the operational window for both polarization and wavelength independence. The calculated dimensions correspond to the best device performance.

4. Conclusions

We have proposed a highly robust 2×2 MMI photonic switch. We have shown that by proper selection of the MMI design, the switch can be made extremely tolerant to perturbations as a result of material modifications

and fabrication errors. By employing this configuration, crosstalk levels better than −20 dB are achievable over a wavelength range of 100 nm while maintaining polarization independence. Moreover, switching speed limitations due to carrier depletion can be removed by taking advantage of the high symmetry of the switch. The switching performance makes this switch an ideal candidate for future wavelength division multiplexing systems.

References

Amann, M.C., S. Illek, C. Schanen and W. Thulke. *IEEE Photon. Technol. Lett.* **1** 253, 1989.
Angulo, Barrios C., V.R. Almeida, R. Panepucci and M. Lipson. *J. Lightwave Technol*. **21** 2332, 2003.
Bennett, B.R., Richard A. Soref and Jesus A. del Alamo. *IEEE J. Quantum. Electron.* **26** 113, 1990.
Duthie, P.J., N. Shaw, M.J. Wale and I. Bennion. *Electron. Lett*. **27** 1747, 1991.
Earnshaw, M.P and D.W.E. Allsopp. *J. Lightwave Technol*. **20** 643, 2002.
Huang, T., Y. Chung, L.A. Coldren and N. Dagli. *IEEE J. Quantum Electron.* **29** 1131, 1993.
Ito, F., M. Matsuura and T. Tanifuji. *IEEE J. Quantum. Electron.* **25** 1677, 1989.
Leuthold, J. and Charles H. Joyner. *J. Lightwave Technol*. **19** 700, 2001.
Levy, D.S., K.H. Park, R. Scarmozzino, R. M. Osgood, C. Dries, P. Studenkov and S. Forrest. *IEEE Photon. Technol. Lett.* **11** 1009, 1999.
Lien, C.H., H.H. Lin, S.W. Weng, H.J. Wang and W.C Chang. *Microwave Opt. Technol. Lett.* **33** 174, 2002.
May-Arrioja, D.A., N. Bickel and P. LiKamWa. *IEEE Photon. Technol. Lett.* **17** 333, 2005.
Nagai, S., G. Morishima, H. Inayoshi and K. Utaka. *J. Lightwave Technol.* **20** 675, 2002.
Nagai, Y., K. Shigihara, H. Saito, H. Watanabe, M. Otsubo and K. Ikeda. *IEEE Photon. Technol. Lett.* **7** 464, 1995.
Schraud, G., G. MÜller, L. Stoll and U. Woff. *Electron. Lett.* **27** 297, 1991.
Shim, J.-I., M. Yamaguchi, P. Delansay and M. Kitamura. *IEEE J. Sel. Top. Quantum. Electron.* **1** 408, 1995.
Soldano, L.B. and E.C.M. Pennings. *J. Lightwave Technol.* **13** 615, 1995.
Themistos, C. and B.M. A. Rahman. *Appl. Optics* **41** 7037, 2002.
Yagi, M., S. Nagai, H. Inayoshi and K. Utaka. *Electron. Lett.* **36** 533, 2000.
Yang, W., A. Gopinath and M. Hibbs-Brenner. *IEEE Photon. Technol. Lett.* **7** 848, 1995.
Yun, I. and K. Hyun. *Microelectron. J.* **31** 635, 2000.